ACADEMIA ROMÂNĂ
Revue Roumaine de Chimie
https://www.icf.ro/rrch/

Rev. Roum. Chim.,
2023, *68*(9), 411–417
DOI: 10.33224/rrch.2023.68.9.01

Papers

SODIUM BENZYL SULFONATE FUNCTIONALIZED-BENTONITE AS A NOVEL ADSORBENT FOR WATER SOFTENING PROCESS

Bahman BEHZADI,[a] Maziar NOEI,[*,b] Alireza AZIMIL,[a] Masoome MIRZAEI[a] and Hossein Anaraki ARDAKANI[b]

[a]Department of Chemical Engineering, Mahshahr Branch, Islamic Azad University, Mahshahr, Iran
[b]Department of Chemistry, Faculty of pharmaceutical chemistry, Tehran Medical Sciences, Islamic Azad University, Tehran, Iran
[c]Department of Chemistry, Mahshahr Branch, Islamic Azad University, Mahshahr, Iran

Received March 12, 2021

In this work, novel Sodium benzyl sulfonate functionalized-bentonite (SBSB) adsorbent was synthesized through the reaction of bentonite with benzyl alcohol and chlorosulfonic acid. The prepared adsorbent was characterized using Low-angle XRD, FT-IR and TGA methods, and applied for the removal of calcium and magnesium ions from water solutions. The effect of contact time and initial hardness concentration on the hardness removal efficiency of the prepared adsorbents were studied. It was found that the adsorption was reached the equilibrium condition within about 60 min, and the maximum adsorption capacity (52.5 $mg \cdot g^{-1}$) was achieved in the hardness of 150 $mg \cdot L^{-1}$. Compared to pristine bentonite, the adsorption efficiency of SBSB was significantly enhanced, which is ascribed to the presence of benzyl sulfonate functional groups on its surface. The adsorption isotherm of calcium and magnesium ions on SBSB was described by Langmuir and its adsorption kinetic behavior followed pseudo-second-order model.

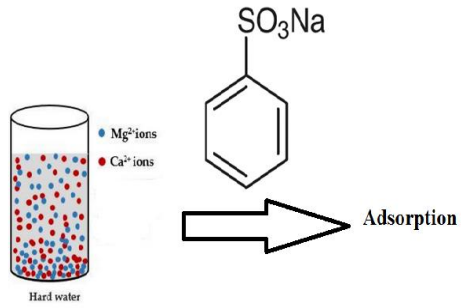

INTRODUCTION

Water hardness is the cause of scale formation in boilers, heat exchangers, cooling towers, and other cooling systems. High hardness in drinking water can result in indigestion and various skin, renal, and hair diseases.[1,2] Various methods are used to remove calcium and magnesium ions to reduce water hardness, including chemical precipitation,[3] microfiltration, nanofiltration, and ultrafiltration,[4,5] reverse osmosis,[6] electrodeionization,[7] adsorption and ion exchange.[8] Among the above-mentioned processes, ion exchange and adsorption approaches are the most important methods for the removal of heavy metals and reducing water hardness.[9,10] The exchange environment has various forms, including natural materials such as sodium chloride salt and zeolites to artificial industrial resins. Several studies have reported various nanosized ion-exchange adsorbents for the removal of calcium and magnesium ions as well as other cations from water. Due to the specific surface area, special morphology, and controlled size distribution, these adsorbents could efficiently remove these cations from water.[11] Modified carbon nanotubes, Single-dimensional titanate nanotubes, zero-dimensional metal oxide

* Corresponding author: Maziar_Noei@hotmail.com; tel.: +986152338579; fax: +986152338579

nanoparticles and iron nanoparticles have a high capacity for adsorbing undesirable ions from water solutions.[12–14] Various studies have attempted to replace the high-cost adsorbents with the cheap ones. These adsorbents include zeolites, diatomite, perlite, clay materials, natural sand, biomass, agricultural waste materials and modified nanopapers.[15–19] Bentonite (BEN), as a cost-effective natural adsorbent, has demonstrated high efficiency in the removal of metal ions through both physical and chemical adsorption mechanisms.[10,11] This adsorbent is abundant and has low preparation costs. However, natural form of BEN has a low adsorption yield, and therefore, its surface required to be modified using appropriate methods to improve its adsorption capacity.[11] More importantly, BEN creates a slurry when it contacts with water, especially in the column method, which can make several problems in its separation from water. Recently, it has been reported that the combination of magnetite with BEN not only could facilitate the separation of adsorbent from the solution due to the induced electromagnetic properties but also increase the adsorption capacity.[10] In the current work, benzyl sulfonic acid functional groups were attached to the surface of bentonite to fabricate an adsorbent with high performance and easy separation ability for water softening process. Sulfonic acid groups were then neutralized using sodium hydroxide, resulting in functionalized bentonite with sodium arene sulfonate. The resultant surface-treated bentonite was served as an ion-exchange adsorbent for the removal of calcium and magnesium ions from aqueous solutions.

RESULTS AND DISCUSSION

Crystalline structure of the samples was determined using low-angle XRD analysis, as represented in Fig. 1a. The diffraction peak at $2\theta = 6.8°$ in the XRD pattern of H-BEN sample is compatible with the interlayer spacing of 1.29 nm in the BEN sample with montmorillonite structure. This peak was shifted toward lower phase angles in SBSB sample, indicating that the distance of the BEN layers was increased due to the diffusion of benzyl alcohol between the layers of BEN.[23–25] FT-IR analysis was conducted to detect the functional groups on the surface of the prepared samples (Fig. 1b). As seen, the peaks at 1098 cm^{-1}, 519 cm^{-1}, and 469 cm^{-1} are due to the stretching vibrational of Si-O bonds and bending vibration of Si-O-Al and Si-O-Si groups, respectively. The broad bands at 1634 cm^{-1} and 3434–3629 cm^{-1} region indicate the bending and vibrational modes of O-H bonds on the surface of BEN, respectively. Importantly, in the FTIR of SBSB sample, the intensity of O-H bonds was reduced, indicating that the H^+ species were effectively exchanged with Na^+ cations. The absorption bands at 2853 cm^{-1} and 2924 cm^{-1} in the FTIR of AS-BEN samples are due to the aliphatic and aromatic C-H bonds which confirm the successful grafting of benzyl alcohol to surface BEN.[20–22] The distinct peaks at 1038 cm^{-1} and 1178 cm^{-1} belong to symmetrical and asymmetrical vibrations of O=S=O bonds. Furthermore, the bands observed at 1036 cm^{-1} and 697 cm^{-1} correspond to the stretching mode of C-S and S-O bonds in Ph-SO_3H structure, respectively.[20–23] TGA plots of the samples are illustrated in Fig. 1c. As seen from TGA plot of BEN sample, two mass reductions were appeared in the temperature range of 30°C to 150°C and above 500°C, which are due to the loss of adsorbed water molecules and dihydroxylation of silicate layers, respectively. For AR-BEN sample, the weight loss in the temperature range of 400°C to 600°C can be due to the decomposition of chemisorbed benzyl alcohol molecules. TGA plot of SBSB sample showed a weight reduction in the temperature range of 250°C to 350°C, which could be assigned to the elimination of sulfonic groups.[20–23] Based on the obtained results, it can be deduced that the BEN adsorbent was successfully functionalized.

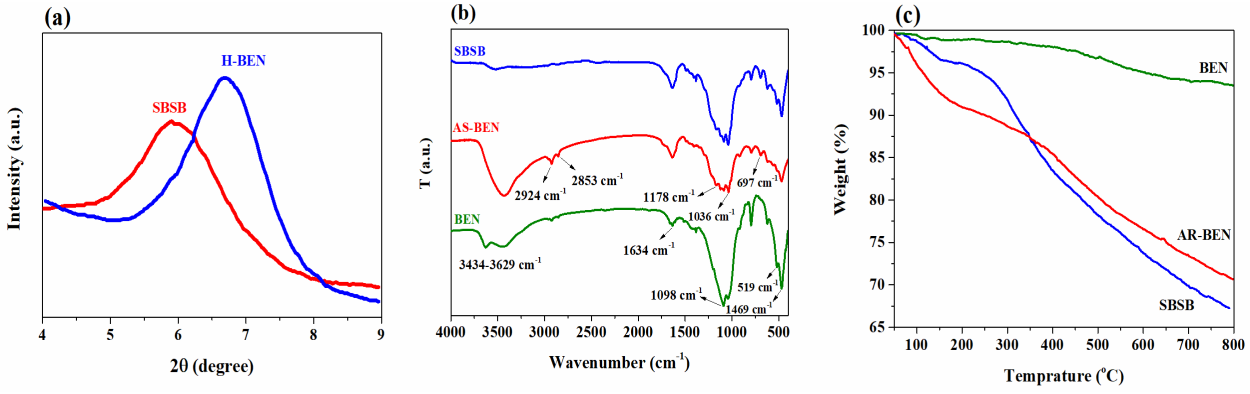

Fig. 1 – a) Low-angle XRD patterns; b) FT-IR spectra; c) TGA plots.

The Effect of contact time on the hardness removal efficiency of BEN and SBSB adsorbents were investigated. As seen in Fig. 2a, the removal efficiency of SBSB and BEN samples was rapidly increased with the increase of the initial ion concentration and then reached the equilibrium condition after 60 min contact time. The sudden drop observed in the removal efficiency of BEN sample after 210 min is related to the release of calcium cations present in its structure into the solution.[11] The hardness removal efficiency of SBSB revealed two-times enhancement compared to bare BEN, which is ascribed to its ion-exchange capability and more density of efficient adsorption sites resulting from the conducted surface modification. Further, the adsorption capacity of SBSB was increased suddenly with increasing the contact time and remained unchanged after 60 min, as can be observed in Fig. 2b.

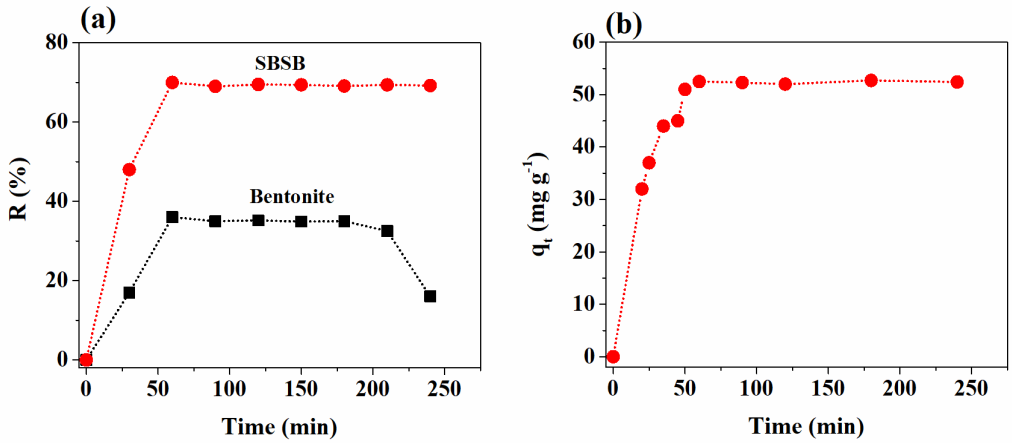

Fig. 2 – a) Hardness removal efficiency of BEN and SBSB; b) adsorption capacity of the SBSB toward water hardness ions at various contact times (conditions: C_i =150 mgL^{-1}, m= 0.1 g, V=50 mL, T= 25 ± 2 ^{0}C and pH=7.0).

Maximum adsorption capacity (q_{max}, mg g^{-1}) is a vital parameter for the investigation of adsorption isotherms. To estimate the q_{max} value of the BEN and SBSB sorbents, the adsorption experiments were conducted at different initial hardness concentrations, as shown in Fig. 3. Clearly, the adsorption capacity was gradually increased with increasing the concentration of Ca^{2+} and Mg^{2+} ions and then reached the q_{max} of approximately 138 mg·g^{-1} and around 70% removal efficiency. Indeed, at high initial concentrations, the removal efficiency was decreased until it reaches ~ 49% at the concentration of 550 mg·L^{-1}. This is because the number of active adsorption sites is limited and these sites are saturated at certain ion concentrations.

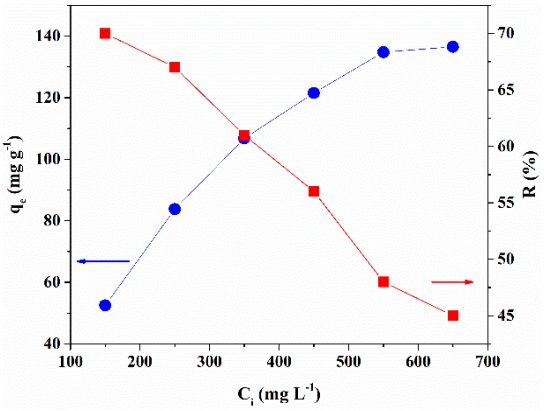

Fig. 3 – The effect of hardness concentration on adsorption capacity and removal efficiency of SBSB sorbent (Conditions: t = 60 min, m = 0.1 g, V = 50 mL, T = 25 ± 2 ˚C and pH = 7.0).

To explore the adsorption mechanism of Ca^{2+} and Mg^{2+} ions on SBSB sorbent, the adsorption data were fitted with Langmuir, Freundlich, Temkin and Dubinin-Radushkevich isotherm

models which are defined as Eqs. (1), (2), (3) and (4), respectively.[24] The corresponding fitted curves are shown in Fig. 4 and the extracted parameters are summarized in Table 1. As is clear, the Langmuir isotherm (R^2 > 0.99) revealed better compatibility with the experimental results compared to the other models, which confirms the single-layer adsorption mechanism. This means that no extra adsorption can occur after the occupation of active adsorption sites. Further, the dimensionless constant of R_L, known as separation factor, is utilized to predict the adsorption efficiency and usability of Langmuir model. It was proved that 0 < R_L< 1 indicates favorable adsorption, while R_L >1, R_L=1 and R_L= 0 represent unfavorable, linear and irreversible adsorption, respectively.[25] In this study, the R_L was calculated to be 0.4 for the adsorption of Ca^{2+} and Mg^{2+} ions on the SBSB, which demonstrates that adsorption efficiency is favorable, suggesting the high performance of the as-prepared adsorbent.

$$\frac{C_e}{q_e} = \frac{\frac{C_e}{q_{\max+1}}}{k_l q_{\max}} \quad (1)$$

$$\log q_e = \log K_f + \frac{1}{n} log C_e \quad (2)$$

$$q_e = BlnA + BlnC_e, B_T = \frac{RT}{B} \quad (3)$$

$$lnq_e = lnq_s - k_{ads}\varepsilon^2,$$

$$\varepsilon = RTln\left(1 + \frac{1}{C_e}\right), \quad (4)$$

$$E = \frac{1}{\sqrt{2k_{ads}}}$$

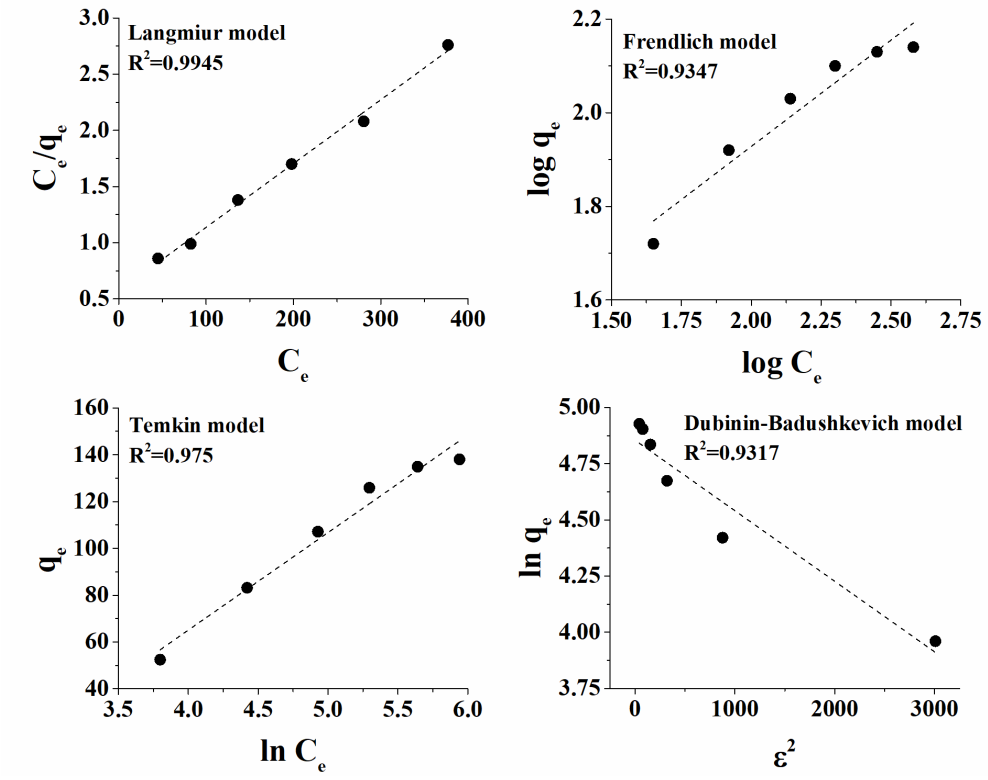

Fig. 4 – Fitting curves of experimental adsorption data with various isotherm models.

Table 1

Extracted parameters of Langmuir, Freundlich, Temkin and Dubinin-Radushkevich models

Model	**Parameters**	***R²***
Langmuir	q_{max} [mg g^{-1}] = 175.5, k_L [min^{-1}] = 0.01, R_L= 0.4	0.9945
Freundlich	k_F [mg/g] = 10.45, 1/*n* = 0.454	0.9347
Temkin	*A* = 0.08, *B* = 41.67, B_T = 59.49	0.975
Dubinin-Radushkevich	q_s [mg g^{-1}] = 128.3, K_{ads} [mol^2 kj^{-2}] =24.36, *E*[$kjmol^{-1}$] =300	0.9317

Kinetic models were explored by measuring the concentration of Ca^{2+} and Mg^{2+} ions at different contact time intervals and the results were fitted using pseudo-first-order, pseudo-second-order, Intra-particle and film diffusion kinetic models, which could be expressed by Eqs. (5), (6), (7) and (8), respectively.[26] Figure 5 shows fitted curves of the experimental adsorption results with the above-mentioned kinetic models, and the extracted parameters were summarized in Table 2. Based on the correlation coefficient values (R^2), it can be concluded that the pseudo-second-order model is more successful than the other kinetic models to explain the adsorption behavior of Ca^{2+} and Mg^{2+} ions over SBSB. Compared to the estimated value of q_e from the pseudo-first-order model (82.4 mg·g^{-1}), the extracted q_e from the pseudo-second-order model (59.9 mg·g^{-1}) is much closer to that obtained through the experimental procedure (52.5 mg·g^{-1}). These observations show that pseudo-second-order kinetic model based on the assumption of ion exchange and chemisorption between adsorbent and solution has good compatibility with the empirical results.[10,11]

$$\frac{dq_t}{dt} = k_1(q_e - q_t) \quad (5)$$

$$\frac{dq_t}{dt} = k_2(q_e - q_t)^2 \quad (6)$$

$$q_t = k_{ip} t^{\frac{1}{2}} + C \quad (7)$$

$$\ln\left(1 - \frac{q_t}{q_e}\right) = -R^l \quad (8)$$

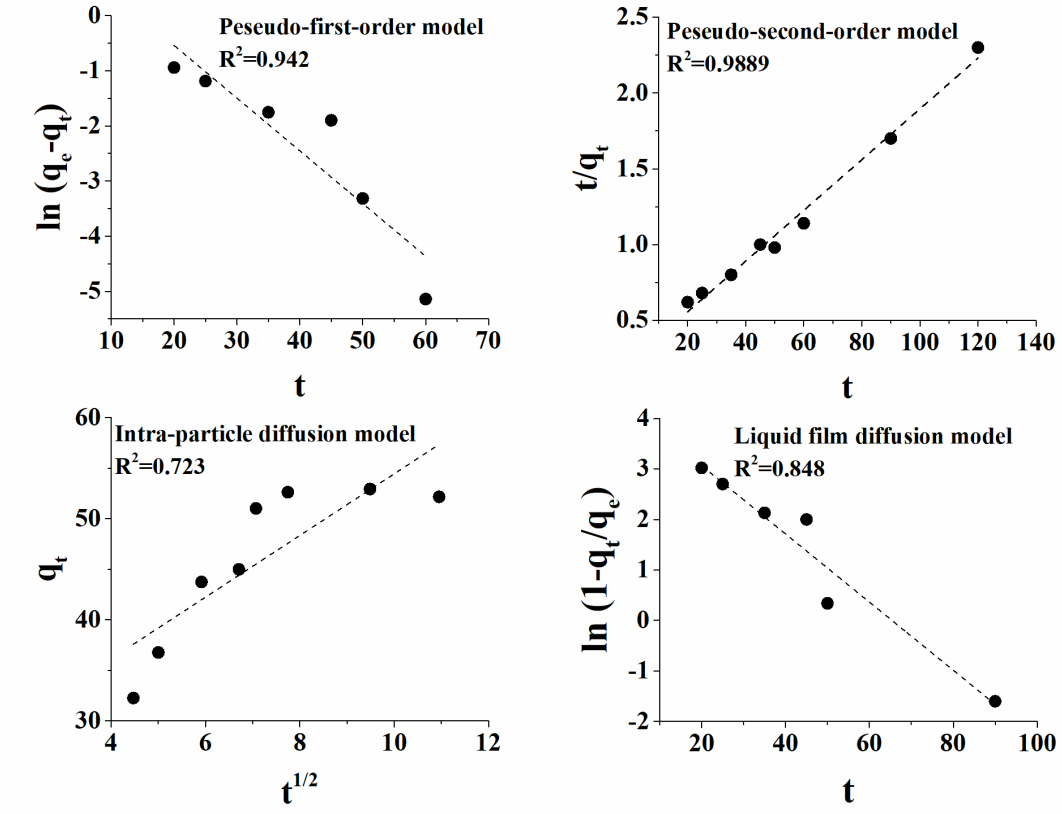

Fig. 5 – Fitting curves of experimental adsorption data with various kinetic models.

Table 2

Extracted kinetic parameters for the adsorption of Ca^{2+} and Mg^{2+} ions on SBSB sorbent

Model	Parameters	R^2
Pseudo-first-order	q_e [mg g^{-1}] = 82.4, k_1 (min^{-1})= 6.75×10^{-2}	0.942
Pseudo-second-order	q_e (mg g^{-1}) = 59.9, K_2 (min^{-1}) = 1.26×10^{-3}	0.989
Intra-particle diffusion	K_{ip} (mg g^{-1}min$^{-1/2}$) = 3.0519, C = 23.938	0.723
Liquid film diffusion	R_l (min^{-1}) = 0.0957	0.848

EXPERIMENTAL

Bentonite, chlorosulfonic acid, HCl, NaOH, and ethylenediaminetetraacetic acid (EDTA) were supplied from Sigma-Aldrich. Calcium nitrate and magnesium nitrate were purchased from Merck, Germany. Absolute ethanol and 2-ethylhexanol were obtained from Bidestan and Tat Chemical companies from Iran, respectively.

IR spectrums of the synthesized solids were recorded by FTIR (JASCO FT-IR-680, Japan) using KBr transparent pills. The crystallinity of the powder samples was studied with a low-angle X-ray diffractometer (XRD, ASENWARE AW-XDM 300, China) using a Cu-Kα radiation source (λ = 1.51418 Å). Thermogravimetric analysis (TGA) of the adsorbent was performed with a Thermoscientific system (Rheometric Scientific, Germany).

To prepare sodium benzyl sulfonate-Functionalized Bentonite (SBSB), Bentonite (BEN) was acid-activated with 0.1 M HCl solution (H-BEN). Then, Arylation was performed on 1.5 g of the H-BEN in the solution containing 7.5 mL benzyl alcohol and 30 mL toluene followed by refluxing at 110 °C for 24 h, and the as-obtained product is labeled as Ar-BEN. Next, Ar-BEN powder was refluxed in the mixture solution of chloroform (10 mL) and chlorosulfonic acid (0.8 mL) at 60 °C for 4 h, and the resultant precipitate is marked as AS-BEN. The AS-BEN was washed with ethanol and water several times and dried at 80°C overnight.[7,8] Finally, the dried AS-BEN was dispersed in 10 mL of 0.1 M NaOH solution and kept at ambient temperature for 24 h to obtain SBSB adsorbent.

Adsorption experiments were conducted as follows: 0.1 g of the as-prepared SBSB sorbent was mixed with 50 mL of the synthetic hard water containing Ca^{2+} and Mg^{2+} ions with various concentrations. The hardness of water samples was measured after defined time intervals using titration with standard EDTA solution. Finally, the adsorption efficiency (R) was calculated according to Eq. (9), where C_0 is the initial concentration and C_e is the equilibrium concentration of metal ions in the operated solution. The adsorption capacity (q_e) was also calculated using Eq. (10), where q_e (mg·g^{-1}) is the amount of adsorbate (mg) adsorbed on 1 g of adsorbent under equilibrium condition, m is the mass of the adsorbent and v is the volume of the solution.

$$R(\%) = \frac{C_0 - Ce}{C_0} \times 100 \quad (9)$$

$$q_e = \frac{(C_0 - Ce)v}{m} \quad (10)$$

CONCLUSIONS

In this study, a cation-exchange adsorbent was fabricated by a chemical grafting method through the reaction of benzyl sulfonic acid groups with natural bentonite. Base on the results obtained from low-angle XRD, FT-IR and TGA analyses, bentonite was successfully functionalized by sodium benzyl sulfonate groups. The as-prepared surface-treated SBSB adsorbent was used for the adsorption of calcium and magnesium ions from aqueous solutions. It was found that Langmuir adsorption isotherm revealed better fitting results compared to the other adsorption models, and the adsorption kinetics followed pseudo-second-order model. The prepared SBSB adsorbent with a maximum adsorption capacity of 175 mg·g^{-1} showed ~1.42 times enhancement in the hardness removal efficiency compared to the pristine bentonite, reflecting that this adsorbent can be used for the softening of industrial and drinking water sources.

REFERENCES

1. E. Ghadamnan, S. R. Nabavi and M. Abbasi, *Journal of Water and Environmental Nanotechnology*, **2019**, *4*, 119.
2. P. Sengupta, *Potential health impacts of hard water*, **2013**, *4*, 8, 866.
3. C. K. Mbamba, S. Tait, X. Flores-Alsina and D. J. Batstone, *Water Research*, **2015**, *85*, 359.
4. H.-Z. Zhang, Z.-L. Xu, H. Ding and Y.-J. Tang, *Desalination*, **2017**, *420*, 158.
5. Y. Wang, L. Ju, F. Xu, L. Tian, R. Jia, W. Song, Y. Li and B. Liu, *Environmental Research*, **2020**, *182*, 109063.
6. Y.-R. Chang, Y.-J. Lee and D.-J. Lee, *J. Taiwan Institute of Chem. Engineers*, **2019**, *94*, 88.
7. Z. Zhang and A. Chen, *Chinese Chem. Lett.*, **2016**, *164*, 107.
8. S. Mountadar, A. Hayani, A. Rich, M. Siniti and S. Tahiri, *Solvent Extraction and Ion Exchange*, **2018**, *36*, 315.
9. M.-L. Cao, Y. Li, H. Yin and S. Shen, *Environm. Int.*, **2019**, *173*, 28.
10. M. M. Alghamdi, A. A. El-Zahhar, A. M. Idris, T. O. Said, T. Sahlabji and A. El Nemr, *Separation and Purification Technology*, **2019**, *224*, 356.
11. N. N. Ab Kadir, M. Shahadat and S. Ismail, *Applied Clay Science*, **2017**, *137*, 168–175.
12. M. A. Tofighy and T. Mohammadi, *Desalination*, **2011**, *268*, 208–213.
13. D. Madarász, I. Szenti, A. Sápi, J. Halász, Á. Kukovecz and Z. Kónya, *Chemical Physics Letters*, **2014**, *591*, 161.
14. P. Saravanan, V. Vinod, B. Sreedhar and R. Sashidhar, *Mater. Sci. Engineering: C.*, **2012**, *32*, 581.
15. S. Bayar, B. A. Fil, R. Boncukcuoglu and A. E. Yilmaz, *J. Chem. Soc. Pakistan*, **2012**, *34*, 841.
16. S. Mohajeri, M. Noei, A. A. Salari, Z. Hoseini, N. Ahmadaghaei and N. Molaei, *Iran. J. Chem. Chem. Eng.*, **2018**, *37*, 39.
17. B. Jayalakshmi, T. Ramachandramoorthy, A. Paulraj, G. Veerapandian, S. M. Kani and G. Naganathan, *World Journal of Pharmacy and Pharmaceutical Sciences (WJPPS)*, **2014**, *3*, 1524.
18. C. Rolence, R. L. Machunda and K. N. Njau, *Research J. Engineering and Appl. Sci.*, **2014**, *3*, 199.
19. A. Mautner, T. Kobkeatthawin, F. Mayer, C. Plessl, S. Gorgieva, V. Kokol and A. Bismarck, *Nanomaterials*, **2019**, *9*, 136.
20. M. Tangestanifard and H.S.Ghaziaskar, *Catalysts*, **2017**, *7*, 211.

21. M. Ghiaci and M. Ghazaie, *Catalysis Communications*, **2016**, *87*, 70.
22. S. Sasikala, S. Meenakshi, S. Bhat and A. Sahu, *Electrochimica Acta*, **2014**, *135*, 232.
23. Y. Leng, J. Zhao, P. Jiang, and D. Lu, *Catalysis Science & Technology*, **2016**, *6*, 875.
24. J. A. Kumar, T. Krithiga, G. Narendrakumar, P. Prakash, K. Balasankar, S. Sathish, D. Prabu, D. P. Pushkala, N. Marraiki, A. G. Ramu and D. Choi, *Environmental Research*, **2022,** *204*, 112070.
25. I. Langmuir, *J. Am. Chem. Soc.*, **1908**, *40*, 1361.
26. H. Qiu, *J.Zhejiang Univ. Sci. A*, **2009**, *10*, 716.